4374 *Chem. Mater.* **2009,** *21,* 4374–4379
DOI:10.1021/cm9005234

CHEMISTRY OF MATERIALS
Article

The Formation of an Almost Full Atomic Monolayer via Surface Modification by N_2O-Plasma in Atomic Layer Deposition of ZrO_2 Thin Films

Seok-Jun Won,[†,‡] Ju-Youn Kim,[‡] Gyu-Jin Choi,[†] Jaeyeong Heo,[†] Cheol Seong Hwang,*[,†] and Hyeong Joon Kim*[,†]

[†]*Department of Materials Science and Engineering, and Inter-University Semiconductor Research Center, Seoul National University, San 56-1, Shillim-Dong, Kwanak-Gu, Seoul 151-744, Korea, and* [‡]*Technology Development Team 2, System-LSI Division, Samsung Electronics Co., Ltd., San 24, Nongseo-Dong, Kiheung-Gu, Yongin-City, Kyungki-Do 449-900, Korea*

Received February 21, 2009. Revised Manuscript Received June 20, 2009

A technique for improving significantly the atomic layer deposition rate of high-*k* ZrO_2 and HfO_2 thin films was developed using a N_2O-plasma oxidant. Even though the process showed much higher growth rate, electrical properties of the dielectric films were similar or superior to those of the film using the conventional O_2-plasma oxidant. From the results of Auger electron spectroscopy and X-ray photoelectron spectroscopy, it was concluded that the nitric oxide species were temporally adsorbed on the surface during the N_2O plasma process and then removed the ligands from the adsorbed metal precursors more effectively, which allowed more precursors to adsorb. In particular, the deposition rate of ZrO_2 thin films (~0.184 nm/cycle) was similar to the full atomic monolayer deposition rate. This phenomenon is expected to be applied to the surface modification of nanostructured materials as well as the improvement in the interface quality of thin films.

1. Introduction

Atomic layer deposition (ALD) has been highlighted as a method for producing one or two-dimensional nanostructures[1−4] as well as for modifying their surfaces because it has very low deposition temperature and precise controllability of the film thickness.[5−9] Atomic layer deposition can control the layer thickness on the atomic scale through alternating injections of the sources and reactants. In the step providing precursors to the substrate, the precursors are initially adsorbed chemically on the surface with the additional precursors being adsorbed physically on the already deposited precursor molecules. Physically adsorbed precursors are desorbed during the subsequent purge step resulting in the growth of one (or subone) atomic layer in the subsequent reactant pulse step. This results in a self-limited growth behavior of the thin films, where the growth rate (GR) is determined solely by the number of reaction sites on the initial surface, regardless of the precursor and reactant doses. However, in most experimental ALD, the thickness GR is usually < 0.1 nm per cycle, which is less than one-half of a full atomic monolayer (0.2−0.3 nm), with the exception of some cases. This suggests that in ALD, the growing layer in a single cycle contains a large number of vacant sites on the surface that are subsequently filled with the adsorbing atoms during the subsequent cycles. The reason why all possible reaction sites on the surface do not chemically adsorb the precursors during a single precursor pulse step is usually attributed to a "steric hindrance effect", where the bulky ligands of the chemically adsorbed precursor molecules at certain reaction sites prevent the adsorption of molecules in the nearby reaction sites.[10] This is a crucial problem of ALD processes because it reduces the GR even further. One of the general problems with ALD is the low GR on account of its layer-by-layer growth nature. Therefore, developing a method that can improve the GR is highly desirable for most ALD processes.

For ALD, the reaction site density on the surface is approximately 1×10^{14} to $7 \times 10^{14}/cm^2$.[11] This is considered to be the upper limit of the adsorbing atom density when a full monolayer is formed during a single

*Corresponding author. E-mail: cheolsh@snu.ac.kr (C.S.H.); thinfilm@snu.ac.kr (H.J.K.).

(1) Triani, G.; Evans, P. J.; Attard, D. J.; Prince, K. E.; Bartlett, J.; Tan, S.; Burford, R. P. *J. Mater. Chem.* **2006**, *16*, 1355.
(2) Fan, H. J.; Knez, M.; Scholz, R.; Nielsch, K.; Pippel, E.; Hesse, D.; Zacharias, M.; Gösele, U. *Nat. Mater.* **2006**, *5*, 627.
(3) Leskelä, M.; Kemell, M.; Kukli, K.; Pore, V.; Santala, E.; Ritalta, M.; Lu, J. *Mater. Sci. Eng.* **2007**, *C27*, 1504.
(4) Daub, M.; Knez, M.; Goesele, U.; Nielsch, K. *J. Appl. Phys.* **2007**, *101*, 09J111.
(5) Farmer, D. B.; Gordon, R. G. *Nano Lett.* **2006**, *6*(4), 699.
(6) Kim, H. W.; Shim, S. H. *Appl. Surf. Sci.* **2006**, *253*, 510.
(7) Xuan, Y.; Wu, Y. Q.; Shen, T.; Capano, M. A.; Cooper, J. A.; Ye, P. D. *Appl. Phys. Lett.* **2008**, *92*, 013101.
(8) Ras, R. H. A.; Kemell, M.; Wit, J.; Ritala, M.; Brinke, G.; Leskelä, M.; Ikkala, O. *Adv. Mater.* **2007**, *19*, 102.
(9) Khare, B. N.; Meyyappan, M.; Kralj, J.; Wilhite, P.; Sisay, M.; Imanaka, H.; Koehne, J.; Baushchlicher, C. W. Jr. *Appl. Phys. Lett.* **2002**, *81*(27), 5237.
(10) Ylilammi, M. *Thin Solid Films* **1996**, *279*, 124.
(11) Alam, M. A.; Green, M. L. *J. Appl. Phys.* **2003**, *94*(5), 3403.

 Published on Web 09/18/2009

cycle of ALD. Whether this can be achieved is dependent on the process conditions and types of precursors, as will be discussed below.

One successful ALD process is the ALD of Al_2O_3 using trimethyl-aluminum (TMA) as the Al-precursor and H_2O or O_3 as the oxidant.[12] The partial pressure of TMA (of which the molecular weight, M, is 114 g) is approximately a few hundred millitorr in a typical deposition system. In the case of a partial pressure of 100 mTorr, the molecular flux onto a growing surface at the typical ALD temperature of 300 °C is calculated to be $\sim 1.37 \times 10^{19}$ molecules/$cm^2 \cdot s$ using the equation: molecular flux $= 3.51 \times 10^{22} \times P/(MT)^{1/2}$, where P(torr) and T(K) are the partial pressure of the precursor and wafer temperature.[13] Therefore, the molecular flux is $\sim 1.37 \times 10^{18}/cm^2$ when TMA is pulsed for 0.1s. Even with a low sticking probability of ~ 0.01, the reaction surface can be completely saturated at a molecular flux of $\sim 1.37 \times 10^{18}/cm^2$. Therefore, when the partial pressure of the precursor is 100 mTorr and the pulse time is 0.1s, the surface saturation with the adsorbing molecules can be completed quickly, provided there are no adverse interfering effects. However, the typical GR of Al_2O_3 thin films by ALD is still $\lesssim 0.1$ nm/cycle[14] even with the high probability of full saturation of the reaction sites because of the high vapor pressure of the precursor.

The situation is even worse for other important high-k oxides, such as HfO_2 and ZrO_2. The most typical Hf and Zr precursors are tetrakis-ethyl-methyl-amino-hafnium (TEMAH) and tetrakis-ethyl-methyl-amino-zirconium (TEMAZ), respectively, of which the partial pressure is < 10 mTorr in a typical deposition system. Although a simple comparison of the partial pressures is a crude way of considering the possible coverage of the reaction sites with the precursors, it is quite evident that a precursor with a low vapor pressure generally requires a much longer pulse time to achieve the saturated GR in ALD. The relatively larger molecular size of the precursor, which is generally necessary to achieve a higher vapor pressure of such relatively heavy metal atoms, would make the steric hindrance effect more severe so that achieving a full monolayer coverage would become more difficult even with a very long precursor pulse time. For these cases, the optimized design to minimize the volume of the ALD chamber is essential for achieving the saturated GR within a reasonable short pulse time (< 1 s).

There are few choices of proper precursors in high-k film ALD. Therefore, the use of an alternative oxidant might be one way of overcoming the low GR problem. The typical oxidants for the ALD of high-k films are H_2O, O_3, and O_2-plasma. However, these oxidants have a limited effect in improving the GR. In this study a plasma-activated N_2O gas was used as the oxidant to grow various high-k films. It was confirmed that the formation of intermediate N-related surface species during one cycle of ALD played a key role in significantly improving the GR. The saturation GR was improved by ~100% by adopting this innovative method.

2. Experimental Section

High-k ZrO_2, HfO_2, and TiO_2 thin films were deposited on Si substrates using an 8"-diameter scale cross-flow type plasma-enhanced ALD (PEALD) system (ASM Genitech Corp.). The deposition temperature and pressure during ALD were 280°C and 3−5 Torr, respectively. A direct plasma with a frequency of 13.56 MHz, and a power of 300−500 W was applied during the oxidant pulse step. TEMAZ, TEMAH, and tetrakis-titanium-isopropoxide (TTIP) were used as the precursors for ZrO_2, HfO_2, and TiO_2 thin films, respectively. O_2 or N_2O was used as the reactant (oxidant). The unit cycle of the PEALD consisted of five steps, "source pulse/source purge/reactant pulse/plasma application/reactant purge". The reactant pulse step was inserted to stabilize the atmosphere of the chamber before generating the plasma. The cycle time of ZrO_2 and HfO_2 deposition was 1/2/0.2/1/0.2 s, and the cycle time of TiO_2 deposition was 1/2/0.5/5/2 s. This specific PEALD has an important advantage in reducing the cycle time of the reactant pulse and purge compared with thermal ALD because reactive species are abruptly generated when the plasma is turned on, which disappears within a few microseconds when the plasma is turned off.

The thickness of the high-k thin films was measured using an ellipsometer with a fixed refractive index value. The area density of Hf and Ti was measured by X-ray fluorescence spectroscopy (XRF). The electrical properties, such as capacitance, leakage current density, and dielectric breakdown, were examined using a Hewlett-Packard 4284, Hewlett-Packard 4194, and Hewlett-Packard 4285. The chemical compositions and surface chemical structures of the high-k thin films were analyzed by Auger electron spectroscopy (AES) and X-ray photoelectron spectroscopy (XPS, Sigma Probe, Thermo VG). Surface roughness was investigated by using atomic force microscopy (AFM, JEOL, JSPM 5200).

3. Results and Discussions

Figure 1a shows the changes in film thickness as a function of the number of ALD cycles of the ZrO_2 thin films when deposited on a Si substrate by O_2-plasma and N_2O-plasma, respectively. The substrate temperature was 280°C. These conditions correspond to the saturated growth conditions for ZrO_2 films. The saturation characteristics of growth rate with respect to the precursor and oxidant pulse time were confirmed by the preliminary experiments. As an example for the saturation behavior, the inset in Figure 1a shows the variation in the growth rate of ZrO_2 films as a function of TEMAZ pulse time where the precursor purge, O_2-plasma pulse, and purge times were 2, 1, and 0.2 s, respectively. The growth rate was almost saturated to 0.1 nm/cycle after the pulse time of ~ 0.4 s. This is a slightly larger value compared to the value determined from the thickness vs number of cycle plots shown below due to the involvement of interfacial layers. Although other saturation characteristics are not shown, all the growth rates reported in this work were saturation growth rates which were confirmed by the

(12) Jakschik, S.; Schroeder, U.; Hecht, T.; Dollinger, G.; Bergmaier, A.; Bartha, J. W. *Mater. Sci. Eng.* **2004**, *B107*, 251.
(13) Ohring, M. *Materials Science of Thin Films*; Academic Press: San Diego, 2002.
(14) Ott, A. W.; McCarley, K. C.; Klaus, J. W.; Way, J. D.; George, S. M. *Appl. Surf. Sci.* **1996**, *107*, 128.

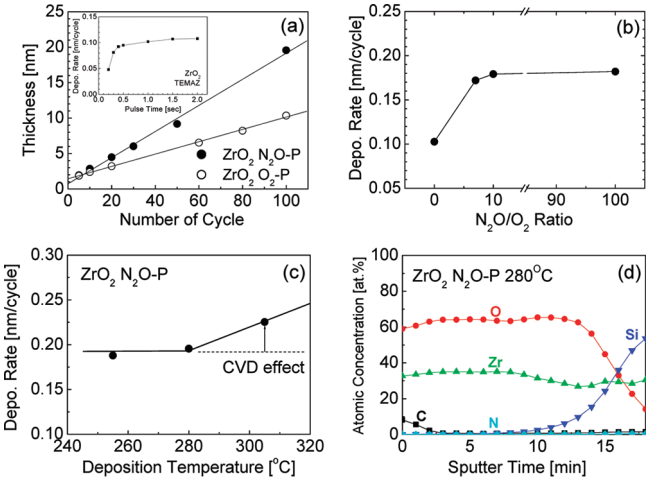

Figure 1. (a) Deposition rates of ZrO_2 films deposited by N_2O plasma and O_2 plasma. (b) Deposition rates of ZrO_2 films as a function of the gas flow ratio of N_2O/O_2. (c) Deposition rates of ZrO_2 films deposited by N_2O plasma as a function of the deposition temperature. (d) AES depth profiles of the ZrO_2 film deposited at 280 °C using N_2O plasma. Nitrogen was not detected in the ZrO_2 film.

preliminary experiments. The GR of the bulk film, which is independent of the presence of interfacial layers, was estimated from the slopes of the best-linear fitted graphs shown in Figure 1a. The N_2O-plasma process shows a GR of 0.184 nm/cycle, which is approximately 2.1 times higher than that (0.087 nm/cycle) of the O_2-plasma process. Because the thickness of the monolayer of bulk ZrO_2 is ~0.2 nm,[15] the high GR of the N_2O-plasma process suggests that an almost fully covered atomic monolayer was formed during a single ALD cycle. Figure 1b shows the change in the GR as a function of the N_2O concentration in the oxidant (the other gas was O_2) mixture. It can be understood that only ~7% N_2O was needed to enhance the GR significantly. In ALD, an increase in GR can be attributed to two factors: an increase in the density of the reactive species and thermal decomposition of the physically adsorbed precursors, i.e. chemical vapor deposition (CVD) effect. It was reported that N_2O gas thermally decomposed through the following two steps; (1) $N_2O \rightarrow N_2 + O$, and (2) $N_2O + O \rightarrow 2NO$.[16] Similar reactions might also occur in a plasma environment. N_2O has a higher dissociation probability in plasma than oxygen because the dissociation energies of N_2-O, $N-NO$, and $O=O$ are 1.67, 4.9, and 5.1 eV, respectively.[16−18] Therefore, even with a small concentration of N_2O gas in the oxidant gas, a much higher density of the active species is generated from N_2O in the chamber, which is believed to be responsible for the enhanced GR shown in panels a and b in Figure 1. The GR was checked at 255, 280, and 305 °C, in order to determine if this increase in GR is due to the thermal decomposition of the precursors and the formation of multiple layers on the surface, as shown in Figure 1c. Although this is not enough data to clearly show the full ALD temperature window, where the GR is independent of deposition temperature, it is quite certain that 280 °C is within the ALD process window for this specific ALD reactor. The ALD reaction using the O_2 and N_2O plasma may proceed via the reaction that is similar to the ALD with O_3 oxidant, where active oxygen atoms are produced and mediate a certain ALD type reaction. The ligands may be removed as CO, CO_2, and H_2O. As H_2O can be produced as the reaction byproduct, OH-ligand mediated ALD reactions can also take part in during the film deposition. Figure 1d shows the AES depth profiles of ZrO_2 thin films deposited using the N_2O plasma. In this analysis, no detectable nitrogen was found in the film. However, it is believed that nitrogen played an important role in achieving a higher GR of the ZrO_2 film during the mean time of ALD cycles, even though it was not incorporated into the film. As a result, a certain type of catalytic effect can be considered for this case.

To check if the higher GR of the film resulted in a deterioration of the electrical performance of the films, the leakage current densities of ZrO_2 thin films deposited by O_2 plasma and N_2O plasma were examined as a function of the applied electrical field ($J-E$ curves), as shown in Figure 2a. Equivalent oxide thicknesses (EOT, $\varepsilon_0 \times \varepsilon_{SiO2} \times A/C$, where ε_0, ε_{SiO2}, A, and C are permittivity in vacuum, dielectric constant of SiO_2 (3.9), electrode area, and capacitance, respectively) of 1.27 and 1.35 nm were measured from the capacitance−voltage ($C-V$) measurements of the films deposited using the N_2O- and O_2-plasma, respectively. The number of ALD cycles for each process was controlled in order to achieve a similar EOT value for the N_2O- and O_2-plasma processes. The ZrO_2 film grown by the N_2O-plasma process does not show any notable degradation in leakage current density, even though the GR was highly improved. This was further confirmed from the expected lifetimes (time to hard breakdown at a certain voltage). The 10 year lifetime was achieved at ~3 V for both films, as shown in Figure 2b.

A similar enhancement effect in the GR of HfO_2 thin films using the N_2O-plasma was also confirmed. Figure 3a shows an approximately 100% increase in the bulk film GR compared to the O_2-plasma case (0.137 nm/cycle for N_2O vs 0.068 nm/cycle for O_2). Panels b and c in Figure 3 show the $J-E$ curves and lifetime expectation, respectively, of the HfO_2 films with a similar EOT but grown under the different plasma conditions. The HfO_2 film grown by the N_2O-plasma process showed a better or similar electrical performance compared to that of the HfO_2 film grown by the O_2-plasma process. The higher GR of the N_2O-plasma process was also observed over the three-dimensional deep hole structured capacitors. The inset transmission electron microscopy (TEM) image in Figure 3d shows the cross-sectional structure of the

(15) Puurunen, R. L.; Vandervorst, W.; Besling, W. F. A.; Richard, O.; Bender, H.; Conard, T.; Zhao, C.; Delabie, A.; Viitanen, M. M.; Ridder, M.; Brongersma, H. H.; Tamminga, Y.; Dao, T.; Win, T.; Verheijen, M.; Kaiser, M.; Tuominen, M. *J. Appl. Phys.* **2004**, *96* (9), 4878.
(16) Tobin, P. J.; Okada, Y.; Ajuria, S. A.; Lakhotia, V.; Feil, W. A.; Hedge, R. I. *J. Appl. Phys.* **1994**, *75*(3), 1811.
(17) Keim, E. G.; Wolterbeek, L.; Van Silfhout, A. *Surf. Sci.* **1987**, *180*, 565.
(18) Bhat, M.; Kim, J.; Yan, J.; Yoon, G. W.; Han, L. K.; Kwong, D. L. *IEEE Electron. Dev. Lett.* **1994**, *15*(10), 421.

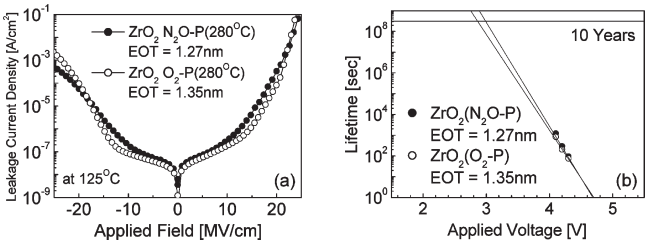

Figure 2. (a) Leakage current densities and (b) TDDB characteristics of ZrO_2 films deposited by N_2O plasma and O_2 plasma. The numbers in parentheses in (a) denote the deposition temperatures. "at 125 °C" in (a) indicates the measurement temperature.

capacitor hole with a diameter and height of 0.25 and 0.8 μm, respectively. In this capacitor, the bottom electrode was a 20 nm thick TiN layer grown by a metal-organic CVD (MOCVD), and the top electrode was composed of sputtered-TiN (the thickness was 40 nm) followed by the deposition of an 80 nm thick TiN film again by MOCVD. Here, the composite $(Zr,Hf)O_2$ film was grown conformally, as expected from the ALD process, with both the N_2O- and O_2-plasma processes (inset TEM image in Figure 3d corresponds to the N_2O-plasma process). The number of ALD cycles was again controlled to achieve a similar EOT of the $(Zr,Hf)O_2$ films using the N_2O- and O_2-plasma processes considering the significantly different GR. The addition of ZrO_2 into HfO_2 leads to a lower EOT than that of pure HfO_2 because of the higher dielectric constant of ZrO_2 while having a better reliability. The ratio of Zr:Hf was ~2.5:1. The almost identical $J-E$ curves (measured at 85 °C) of the two films grown on the deep hole structured capacitors shown in Figure 3d suggest that the higher GR was conformal all over the hole structure. The results show that the GR of ZrO_2 and HfO_2 films was improved by as much as 100% by adopting N_2O-plasma without sacrificing the electrical performance. The following discusses the possible reasons for this improvement.

To confirm if nitrogen (N) is temporarily present on the growing surface at a certain moment of ALD (most probably immediately after the N_2O-plasma step), we used surface sensitive XPS to detect N after the N_2O-plasma step of the growing film. Although the XPS was not performed in situ, N might be detected by XPS because N is almost never adsorbed on the surface from air at room temperature. Furthermore, to exclude the possible incorporation of N from the amino ligands of the TEMAH or TEMAZ, we used N-free TTIP to grow TiO_2 films. However, regardless of the types of oxidants, N 1s XP spectra related to nitric oxide were hardly detected when the film was grown on the flat Si substrate. This may be due to the very lower density of surface N even if they actually remain on the film surface. Therefore, in order to increase the possibility of detecting N on the film surface, a porous low-k SiOC film was used as a substrate for the TiO_2 ALD. The low-k film with a

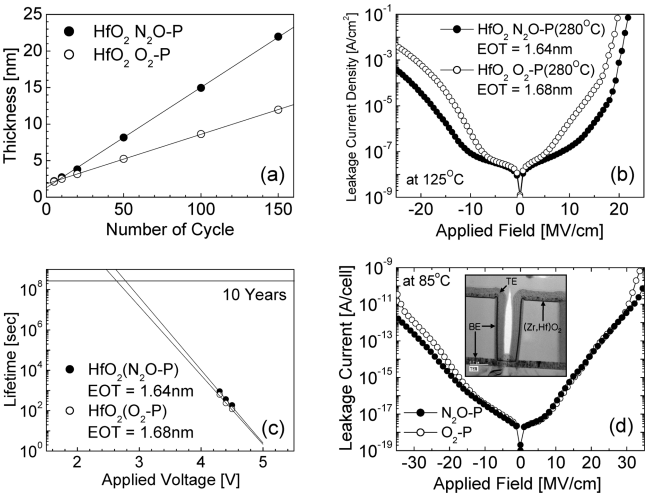

Figure 3. (a) Deposition rates, (b) leakage current densities, and (c) TDDB characteristics of HfO_2 films deposited by N_2O plasma and O_2 plasma. (d) Leakage current densities of $(Zr,Hf)O_2$ composite films in the three-dimensional capacitor structure. The inset of (d) shows a TEM image of the capacitor structure. BE and TE mean the bottom and top electrode, respectively. The dark line following the contour of a concave hole displays the $(Zr,Hf)O_2$ composite film. "at 85 °C" in (d) indicates the measurement temperature.

dielectric constant of 2.5 was exposed to ultraviolet lamps (100 °C, 5 min) in order to generate many open pores with the appropriate diameter (~1 nm).[19] Only one ALD cycle of the TiO_2 film was performed on the standard Si and low-k substrates, and the amount of deposited Ti was estimated by XRF. The relative amount of Ti on the porous low-k substrate was ~15 times higher than that on the Si substrate. This suggests that the high specific surface area of the porous low-k substrate was quite effective in increasing the amount of surface adsorption.

Therefore, the surface chemistry of the porous low-k substrate after 1 cycle of TiO_2 deposition using N_2O-plasma was examined by XPS. Here, the final step before the XPS was the purge of N_2O-plasma. Figure 4a shows the N 1s XPS spectra of the low-k substrate (0 cycle) and after the 1 cycle of TiO_2 deposition. The increase of the N signal was observed, which confirms that nitrogen was adsorbed after the 1 cycle of ALD TiO_2. The density of N was approximately similar to that of titanium when calculated in consideration of atomic sensitivity factors. The binding energy of the N 1s peak (399−400 eV) was close to that of a N atom bonded to an O atom.[20] However, the AES depth profiles of Figure 1d showed no nitrogen in the final film. The detection limit of XPS and AES is similar (~0.5%). This suggests that N exists only temporarily on the film surface. Figure 4b−d show XPS spectra of silicon, carbon, and oxygen, respectively, before and after 1 cycle of TiO_2 deposition. In silicon, the peak intensity around 104 eV from SiOH was drastically reduced after 1 cycle of TiO_2 deposition. In the range of 101.5 to 103.5 eV related to SiO_xC_y, the intensity of the relatively high binding energy increases, which means that carbon atoms bonded to silicon atoms are replaced

(19) Heo, J.; Won, S.-J.; Eom, D.; Lee, S. Y.; Ahn, Y. B.; Hwang, C. S.; Kim, H. J. *Electrochem. Solid-State Lett.* **2008**, *11*(8), H210.

(20) Sandell, A.; Nilsson, A.; Mårtensson, N. *Surf. Sci.* **1991**, *251*/*252*, 971.

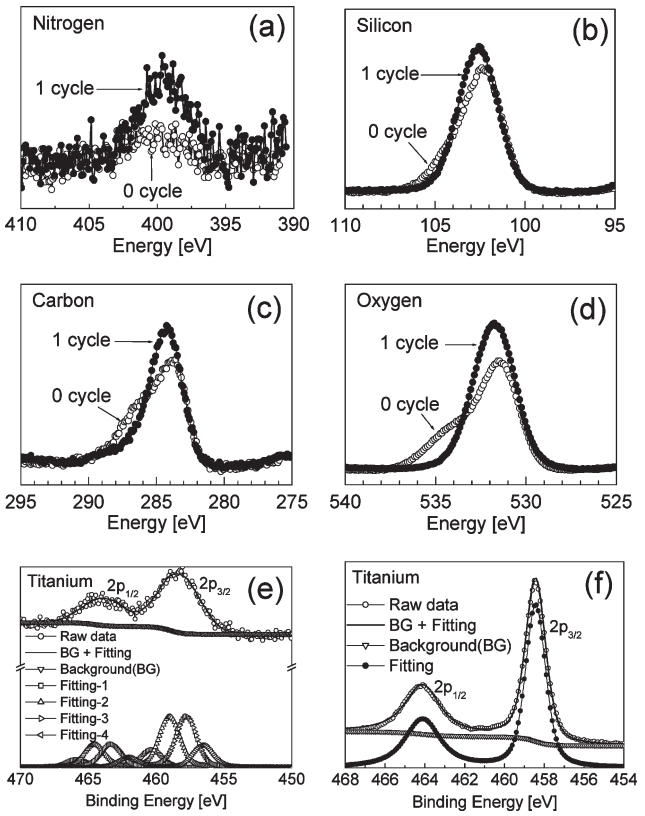

Figure 4. (a) XPS N 1s peaks, (b) XPS Si 2p peaks, (c) XPS C 1s peaks, (d) XPS O 2p peaks, and (e) XPS Ti 2p peaks for 0 and 1 cycle of TiO_2 on the UV-treated low-k film. (f) XPS Ti 2p peaks for the 5.5 nm thick TiO_2 film on the normal Si substrate.

partially by oxygen atoms. In carbon, the peak intensities of 286 to 289 eV related to carbonates (CO, COH) and 283.5 eV from SiC decreased significantly after 1 cycle of TiO_2 deposition. In oxygen, the peak intensities from Si−O−H (534.5−535.5 eV) were reduced significantly after 1 cycle of TiO_2 deposition. In the range of 530−533 eV, the peak intensity increased after 1 cycle of TiO_2 deposition because new peaks from Ti−O−N (530−531 eV), C−O−N (532 eV), and Ti−O−Ti (530−531 eV) appear, even though the peaks for C−O−H (530.5−531.5 eV) and Si−O−C (531−532 eV) are weakened. However, because of the limited resolution of the XPS instrument, the O 1s peak cannot evidently prove the presence of N on the film surface.

Panels e and f in Figure 4 show the Ti 2p XP spectra and their deconvolution results for the 1 cycle ALD TiO_2 on the porous low-*k* substrate and the 5.5 nm thick TiO_2 film on the normal Si substrate, respectively. Deconvolution results of the Ti 2p spectrum from the thinner film suggest that the layer is composed of mainly TiO_2 (peak at ~459 eV) and Ti−O−N (peak at ~458 eV) with a minor amount of Ti−N (peak at ~456 eV) and possible Ti−Si−O (peak at ~461 eV). The major presence of Ti−O−N coincides well with the N 1s result in Figure 4a. The high affinity of Ti to N may result in the partial formation of Ti−N bodings. The spectrum from the thick TiO_2 films was exclusively composed of Ti^{4+} state signal, suggesting that the Ti−N bonding was hardly remained. Therefore, it can be understood that N is intermediately involved during the film growth but readily removed during the subsequent steps by either the ligand exchange reaction or oxidation.

AFM (data not shown) revealed that the surface morphology of the PEALD TiO_2 film was very smooth. A root-mean-squared roughness of ~ 0.2 nm was achieved from a 5 nm thick TiO_2 film (scan area $2 \times 2\ \mu m^2$), which is similar to the value of the film grown by a thermal ALD using the same precursor and H_2O oxidant.

From these experimental results, a model can be assumed to explain the ALD behavior of ZrO_2 (HfO_2 too) thin films depending on the types of oxidants. In the case of O_2-plasma, active oxygen on the surface removes some of the ligands from the metal precursors, but there could be a high proportion of unoccupied reaction sites. This originates mainly from the steric hindrance effect of the residual bulky ligands which are still attached to the adsorbed metal ions. The bulkiness of these remaining ligands precludes the chemisorption of another precursor molecule at the adjacent adsorption sites. For this case, the total ALD process is just a repeat of approximately half monolayer growth of one ALD cycle.

On the other hand, the surface N−O groups in the case of N_2O-plasma are believed to play a key role in improving the GR during the precursor pulse step. Similar ligand exchange reaction occurs when the precursor molecules approach the surface with the N−O groups and active oxygen atoms, and some of the ligands are removed by the chemical reaction as in the case of the O_2-plasma ALD. However, in this case, N ions around the adsorbed precursors may contribute to further chemical reactions that remove the residual ligands from the adsorbed metal ions further. The active N atoms react with the remaining ligands and make the adsorbed precursor molecules retain less ligands. This would reduce the steric hindrance effect during the precursor pulse step and increase the chemical adsorption of the precursor molecules. Therefore, with the favorable surface structure for the precursor adsorption wit the N_2O plasma almost full monolayer coverage can be attained.

Another important point for this type of reaction route is that there is no possibility of multilayer formation. This is because the temperature is not high enough to induce thermal decomposition of the precursor molecules without any surface catalytic reaction. Therefore, the ligands bound to the incoming precursor molecules are rarely dissociated, resulting in little adsorption on the predeposited metal ions which are now free of ligands and active species. Even a small amount of weakly bound molecules to the metal ions by physisorption are easily removed by the subsequent purge step. A more detailed experimental and theoretical study will be needed, particularly for the precursor adsorption step in the N_2O-plasma case. However, the hypothesis made in this study has firm ground considering the well-matched experimental results.

4. Conclusions

ALD of ZrO_2 and HfO_2 using N_2O-plasma resulted in a significant increase (by $\gtrsim$100%) in deposition rate

compared with the ALD with O_2-plasma. In particular, the growth rate of ZrO_2 (0.184 nm/cycle) achieved by the N_2O-plasma process in this study was very close to the ideal monolayer growth rate (~0.2 nm). This suggests that the steric hindrance effect, which is normally the cause of the suppressed growth rate in ALD, was overcome during N_2O-plasma ALD. The active N atoms of the N−O groups immediately after the N_2O-plasma step remove the bulky amino ligands of the precursors more efficiently at the subsequent precursor pulse step and catalyze full coverage of the adsorption sites. This phenomenon is expected to greatly assist in the surface modification of nanostructures and the improvement in interface qualities of thin films.

Acknowledgment. This work was supported by the Korea Science and Engineering Foundation (KOSEF) grant funded by the Korea government (MEST) (R17-2008-043-01001-0), system IC 2010 project, IT R&D program of MKE/IITA (Contract 2009-F-013-01), and World Class University program through the Korea Science and Engineering Foundation funded by the Ministry of Education, Science and Technology (R31-2008-000-10075-0) of the Korean government.